FULL PAPER

BJC

British Journal of Cancer (2014) 111, 807–816 | doi: 10.1038/bjc.2014.372

Keywords: *HOX* genes; HOXD10; HNSCC; head and neck; metastasis; AMOT-p80; miR-146a

The roles of HOXD10 in the development and progression of head and neck squamous cell carcinoma (HNSCC)

F Hakami[1,2], L Darda[1], P Stafford[1], P Woll[3], D W Lambert[1] and K D Hunter*[,1,4]

[1]*Unit of Oral & Maxillofacial Pathology, School of Clinical Dentistry, University of Sheffield, Sheffield S10 2TA, UK;* [2]*Department of Pathology and Laboratory Medicine, King Abdulaziz Medical City-WR, Jeddah, Saudi Arabia;* [3]*Academic Unit of Clinical Oncology, University of Sheffield, Sheffield S10 2SJ, UK and* [4]*Department of Oral Pathology and Biology, University of Pretoria, Pretoria, South Africa*

Background: *HOX* gene expression is altered in many cancers; previous microarray revealed changes in *HOX* gene expression in head and neck squamous cell carcinoma (HNSCC), particularly HOXD10.

Methods: HOXD10 expression was assessed by qPCR and immunoblotting *in vitro* and by immunohistochemistry (IHC) in tissues. Low-expressing cells were stably transfected with HOXD10 and the phenotype assessed with MTS, migration and adhesion assays and compared with the effects of siRNA knockdown in high-HOXD10-expressing cells. Novel HOXD10 targets were identified using expression microarrays, confirmed by reporter assay, and validated in tissues using IHC.

Results: HOXD10 expression was low in NOKs, high in most primary tumour cells, and low in lymph node metastasis cells, a pattern confirmed using IHC in tissues. Overexpression of HOXD10 decreased cell invasion but increased proliferation, adhesion and migration, with knockdown causing reciprocal effects. There was no consistent effect on apoptosis. Microarray analysis identified several putative HOXD10-responsive genes, including angiomotin (AMOT-p80) and miR-146a. These were confirmed as HOXD10 targets by reporter assay. Manipulation of AMOT-p80 expression resulted in phenotypic changes similar to those on manipulation of HOXD10 expression.

Conclusions: HOXD10 expression varies by stage of disease and produces differential effects: high expression giving cancer cells a proliferative and migratory advantage, and low expression may support invasion/metastasis, in part, by modulating AMOT-p80 levels.

Alterations in the genome and transcriptome of head and neck squamous cell carcinoma (HNSCC) are variable and related to the cancer site and stage. This heterogeneity has hindered the identification of molecular alterations that could be exploited as therapeutic targets in HNSCC. The prognosis for patients with HNSCC remains poor for the majority of patients who present at an advanced stage of disease (Leemans *et al*, 2011). Recent advances in the genomic characterisation of HNSCC have identified a number of potential somatic drivers, including NOTCH; however, these are not ubiquitous and subclassification of HNSCC will be required as further detail emerges (Agrawal *et al*, 2011; Pickering *et al*, 2013). It is not yet known whether alterations in these newly identified oncogenic drivers are related to disease severity or clinical outcome in HNSCC.

Our previous transcriptomic analysis of cell cultures from all stages of HNSCC development identified consistent alterations including dysregulation of expression of a number of HOX genes (Hunter *et al*, 2006), one of which was *HOXD10*. HOX genes form a large group of 39 homeodomain-containing transcription factors, found within four clusters in the genome (A, B, C and D), which

*Correspondence: Dr KD Hunter; E-mail: k.hunter@sheffield.ac.uk

Received 13 February 2014; revised 4 June 2014; accepted 9 June 2014; published online 10 July 2014

are involved in embryonic development and also have a role in stem cell function (Picchi *et al*, 2013). Alterations in expression of HOX genes have been identified in a number of cancers, including haematolymphoid/leukaemias, breast and lung cancer (Abe *et al*, 2006; Rice and Licht, 2007; Gilbert *et al*, 2010).

Given their wide range of functions, it is not surprising that HOX genes may be either silenced or overexpressed in cancer. The effects of this aberrant expression in tumour cells include alterations in differentiation, apoptosis and receptor signalling pathways, and have been associated with control of EMT and promotion or inhibition of invasion (Wu *et al*, 2006; Wardwell-Ozgo *et al*, 2014). Control of expression is complex and, for many HOX genes, has not been fully elucidated; however, epigenetic control and the action of microRNAs and other non-coding RNAs, such as HOTAIR, have been demonstrated (Rinn *et al*, 2007). Furthermore, the similarity in function between the paralogous groups of HOX genes introduces an element of functional redundancy, yet it is clear that the functions are not completely interchangeable between paralogues (Eklund, 2007). This indicates that, whereas HOX genes present potential therapeutic targets, significant challenges remain. Nevertheless, a number of small molecular inhibitors of the interaction between HOX genes and their cofactor PBX have been developed, including HXR9 (Morgan *et al*, 2012). Identification of consistent changes in specific HOX genes in particular cancers may present novel therapeutic targets or prognostic markers that can be exploited to improve clinical outcomes.

As the preliminary array data suggested increased expression of HOXD10 in SCC cells when compared with normal keratinocytes, this study aimed to validate this observation and understand the role high HOXD10 expression may have in HNSCC development.

MATERIALS AND METHODS

Cell Culture. Head and neck squamous cell carcinoma cell lines, oral pre-malignant (OPL), primary normal oral keratinocytes (NOKs) and immortalised normal oral keratinocytes (Supplementary Table S3) were maintained in KGM (DMEM supplemented with 23% Ham's F-12, 10% FCS, L-glutamine (2 mM), adenine (0.18 mM), hydrocortisone (0.5 $\mu g\,ml^{-1}$) and insulin (5 $\mu g\,ml^{-1}$; Sigma Aldrich, Cambridge, UK) at 37 °C and 5% CO_2. Primary NOKs were isolated as previously described (Hearnden *et al*, 2009).

RNA extraction and qPCR. Total RNA was extracted using the ISOLATE RNA mini kit (Bioline Reagents Ltd, London, UK) before quantification and purity assessment (A260/280 $\geqslant$ 1.9) using NanoDrop Spectrophotometer (Fisher Scientific, Loughborough, UK). cDNA was generated using the High Capacity cDNA Reverse Transcription kit (Life Technologies, Paisley, UK) with random primers or miR-specific stem–loop primers (Life Technologies). TaqMan probes and primers (Life Technologies) or primers for SYBR green chemistry (Sigma AldrichSupplementary Table S3) were used to amplify target sequences using qPCR (7900HT thermocycler, Life Technologies). Data were analysed using the RQ Manager 1.2.1 software (Life Technologies).

Antibodies. Antibodies used were goat polyclonal anti-HOXD10 (Santa Cruz Biotechnology, Dallas, TX, USA), rabbit polyclonal anti-HOXD10, rabbit polyclonal anti-AMOT-p80 (both Abcam, Cambridge, UK) and mouse monoclonal anti-β-actin (Sigma Aldrich), anti-goat IgG horseradish peroxidase (HRP; Amersham Ltd, Amersham, UK), anti-rabbit IgG HRP (New England Biolabs, Hitchin, UK) and anti-mouse IgG HRP (Cell Signalling, Hitchin, UK).

Western blotting. Cell pellets were lysed using RIPA buffer (Sigma Aldrich) containing protease and phosphatase inhibitors (Roche, West Sussex, UK) and extracted proteins quantified using the BCA method (Smith *et al*, 1985). Protein extracts (100 μg) were loaded onto 12% (v/v) SDS-PAGE, followed by wet transfer to nitrocellulose. Following incubation in blocking buffer (5% milk and 3% BSA in TBS containing 0.05% Tween-20) for 1 h membranes were incubated overnight at 4 °C with anti-HOXD10 (1 : 250) or AMOT-p80 (1 : 250) antibodies. Membranes were incubated in anti-goat IgG HRP (1 : 50 000) or anti-rabbit IgG HRP (1 : 3000) antibodies for 1 h at room temperature and developed with SuperSignal west pico chemiluminescent substrate (Fisher Scientific).

Immunohistochemistry (IHC). HOXD10 protein expression was assessed in a tissue microarray containing normal oral mucosa, OPL, primary HNSCC and metastases. AMOT-p80 expression was assessed in a smaller subpanel of normal and HNSCC tissues. Microwave or pressure cooker antigen retrieval was used and samples were incubated with the primary antibody, rabbit anti-HOXD10 (1 : 50) or rabbit anti-AMOT-p80 (1 : 50), overnight at 4 °C. Vectastain Elite ABC Rabbit IgG kit (Vector Ltd, Peterborough, UK) was used for the secondary antibody step followed by colour development using DAB. Specificity of the antibody was assessed by pre-adsorption with the immunogenic peptide (Abcam). Staining was assessed using the Quickscore method (Detre *et al*, 1995).

HOXD10 and AMOT-p80 plasmid construction. Primers amplifying the coding regions of HOXD10 and AMOT-p80 included a CACC sequence to aid the insertion into pcDNA3.1-TOPO mammalian expressing vector (Life Technologies); HOXD10 forward: 5′-CACCATGTCCTTTCCCAACAGCT-3′, reverse: 5′-CTAAGAAAACGTGAGGTTGGCGG-3′, AMOT-p80 forward: 5′-CACCATGCCTCGGGCTCAGCCATCCTC-3', reverse: 5′- TTAG ATGAGATATTCCACCATCTCTGCATCAGGCTCTTGTC-3′. Successful cloning of target sequences was confirmed by sequencing.

Plasmid, shRNA and siRNA transfection. Cells were transfected in six-well plates with pcDNA3.1-control, pcDNA3.1-HOXD10, pcDNA3.1-AMOT, control shRNA or HOXD10 shRNA plasmids DNA (1 μg per well) using FuGENE HD (Promega, Southampton, UK), whereas HOXD10 siRNA (OriGene, Rockville, MD, USA) transfection was carried out at 50 nM final concentration with Oligofectamine (Invitrogen, Loughborough, UK), as per the manufacturer's protocol. Following transfection, cells were incubated for 48–72 h in their normal media before use in phenotypic or gene expression analyses. Stably transfected cells were selected using G418 (400 $\mu g\,ml^{-1}$; Fisher Scientific) in a 12-well plate for 2 weeks. Selected colonies were expanded and cells were grown in antibiotic-containing media to maintain selection pressure. Transfection efficiency was confirmed using qPCR and western blotting.

Proliferation and apoptosis assays. Cells were seeded (4000 cells per well) in a 96-well plate in triplicate for each time point in DMEM supplemented with 10% (v/v) FCS. At each time point, wells were washed with PBS before adding 100 μl serum-free DMEM medium and MTS reagent (Promega). Absorbance was read at 490 nm using a microplate spectrophotometer (Tecan Ltd, Theale, UK).

Apoptotic cells were quantified using the TACS Annexin V-FITC Apoptosis Detection Kit (R&D systems, Abingdon, UK). Cells were cultured in tissue culture flasks in their respective medium until they are 80% confluent, trypsinised and 5×10^5 cells transferred to a microtube. Cells were washed in ice-cold PBS containing 0.1% BSA, resuspended in binding buffer and incubated with Annexin V-FITC and propidium iodide according to the

manufacturer's instructions. Cells were analysed using a LSR II flow cytometer (BD Biosciences, San Jose, CA, USA).

Adhesion assay. A 96-well plate was coated with 0.1% (w/v) fibronectin (Sigma Aldrich) diluted in PBS and kept overnight at 4 °C. On the following day, wells were washed with PBS and incubated with DMEM containing 1% (w/v) BSA for 1 h. Cells (30 000 cells per well) were seeded in serum-free DMEM medium and incubated for 1 h at 37 °C. Non-adherent cells were removed by washing with PBS before adding 100 μl serum-free DMEM medium and MTS reagent, and absorbance was measured as described.

Transwell migration and invasion assays. To assess migration, 60 000 cells, serum-starved for 24 h, resuspended in DMEM with 0.1% (w/v) BSA and placed in the top chamber of a 24-well Transwell insert (8 μM: BD Biosciences, Oxford, UK). DMEM was added to the bottom well with 2% (v/v) FCS and incubated overnight at 37 °C for 16 h. Migrated cells were stained with crystal violet and counted. To assess cell invasion, a similar protocol was followed with prior coating of the membrane with 100 μl of growth factor-reduced Matrigel (BD Biosciences) diluted in PBS (1 : 45). Mitomycin C was used at a concentration of 1 μg ml^{-1} at both the cell suspension and at the chemoattractant-containing medium in the lower chamber to stop any cell division during the assay.

Agilent microarray. Total RNA was extracted from triplicate cultures of B22 and D19 cells stably transfected with either pcDNA3.1-HOXD10 or pcDNA3.1-control, and T5 and D35 cells transfected with either HOXD10 siRNA or scrambled siRNA control. RNA quality was assessed using an Agilent Bioanalyser (28 s:18 s $\geqslant$ 2 : 1 and RIN = 10). Sample labelling was carried out as per the manufacturer's protocol before hybridisation onto SurePrintG3 Human Oligo arrays (Agilent, Santa Clara, CA, USA). After 17 h, hybridised slides scanned at 3-μm resolution using Agilent C Microarray Scanner. Data were loaded into Genespring (version 12.5), normalised by the Quartile method and analysed using one-way ANOVA (Welch) with Benjamini–Hochberg correction to identify significantly differentially expressed genes with a fold change >2.

The list of significantly differentially expressed genes was filtered using criteria to enrich for putative targets of HOXD10. First, genes that showed reciprocal changes in expression with HOXD10 overexpression and knockdown were selected. Next, the promoter regions of the remaining genes were detected and screened for HOXD10-binding sites using PROMO online algorithm (Messeguer *et al*, 2002) (http://alggen.lsi.upc.es/cgi-bin/promo_v3/promo/promoinit.cgi?dirDB=TF_8.3). Last, the overall pattern of expression was assessed and compared with HOXD10 expression in a cell panel.

Cloning of wild-type and mutated AMOT-p80 and miR-146a promoters. The putative promoter regions of AMOT-p80 and miR-146a were identified using *in silico* analysis using http://rulai.cshl.edu/cgi-bin/CSHLmpd2/promExtract.pl?species=Human (Zhang, 2003), http://biowulf.bu.edu/zlab/PromoSer/ (Halees *et al*, 2003) and http://www.genomatix.de/solutions/genomatix-software-suite.html (Cartharius *et al*, 2005). To clone the promoter sequences into pGL3-basic luciferase reporter vector, sequences of *Xho*I and *Hind*III restriction sites were added to forward and reverse primers, respectively (restriction sites underlined): AMOT-p80 promoter forward: 5′-TGCTAACTCTCGAGAGTCAACTTCATATCCACC CCCAAAA-3′, reverse: 5′-TACGCCAAGCTTACGACCAAGTT CATGCCACCAT-3′, miR-146a promoter forward: 5′-AAAA TTCTCGAGTTGAAAAGCCAACAGGCTCATTGG-3′, reverse: 5′-CAAATTTAAGCTTCCACTCCAATCGGCCCTGCT-3′.

HOXD10-binding sites in AMOT-p80 and miR-146a were predicted using PROMO algorithm: http://alggen.lsi.upc.es/cgi-bin/promo_v3/promo/promoinit.cgi?dirDB=TF_8.3 (Messeguer *et al*, 2002). Using the mutagenic PCR method, random nucleotides in the binding site were substituted with different nucleotides to impair HOXD10 binding. pGL3-AMOT and pGL3-miR-146a wild-type (WT) sequence was used as the templates in this PCR. The primers used for mutation of the HOXD10-binding site in addition to the cloning forward and reverse primers were as follows: (mutated bases in bold): AMOT-p80 mutagenic forward: 5′-CACAATAGCCTCTTGTTTAGT**CC**TATTAATTTTGAGGGC GGGTGG-3′, reverse: 5′-CCACCCGCCCTCAAAATTAATA **GG**ACTAAACAAGAGGCTATTGTG-3′, miR-146a mutagenic forward: 5′-AGGGTGTGGAAATGGAATA**TTT**GCATATGCAA ATAGGCCTT-3′, reverse: 5′-AAGGCCTATTTGCATATGC**AAA** TATTCCATTTCCACACCCT-3′. Successful cloning was confirmed by sequencing.

Dual luciferase reporter (DLR) assay. Cloned pGL3-AMOT and pGL3-miR-146a wild-type (WT) and mutated promoters were transfected using FuGENE HD (Promega) into cells stably expressing pcDNA3.1-HOXD10 DNA or pcDNA3.1-control. To confirm transfection efficacy and to normalise the firefly luciferase expression, constructs were co-transfected with a pRL-TK *Renilla* internal control vector in a ratio of 1 : 10. Forty-eight hours post transfection, cells were lysed and expression levels of firefly and *Renilla* luciferase were determined using the DLR assay kit (Promega) and a GloMax luminometer (Promega) as per the manufacturer's instructions.

Statistical analysis. Non-parametric Kruskal–Wallis test was performed on the IHC scoring for HOXD10 in SPSS (IBM, New York, NY, USA). One-way ANOVA (Welch) was used to identify differentially expressed genes in the microarray data using Benjamini–Hochberg correction. Otherwise, Student's *t*-test was used, unless otherwise stated. Differences were considered statistically significant if $P \leqslant 0.05$.

Ethics. Ethics approval for the use of tissues was obtained from The West Glasgow LREC (08/S0709/70). Ethical approval for the NOK primary cultures used was obtained from Sheffield LREC (09/H1308/66).

RESULTS

HOXD10 expression in HNSCC. Validation of the initial microarray data using qPCR and WB demonstrated high HOXD10 expression in cells from primary HNSCCs compared with NOKs; however, this elevated expression was not observed in cell cultures from lymph node metastases, B22 and TR146 (Figure 1A and Supplementary Figure S1). Expression in the cultures from OPLs was variable, although some – for example, D35 – did express HOXD10 at high levels. No clear relationship between the static level of expression of HOXD10 and that of known interacting molecules, such as miR-7, miR-10b and IGFBP3, was seen (Supplementary Figure S2).

In tissues, HOXD10 was expressed in the nucleus and the cytoplasm. This is similar to reports of a number of other HOX genes (Abe *et al*, 2006) and may represent shuttling between the nucleus and the cytoplasm (Ziegler and Ghosh, 2005). Analysis of HOXD10 expression in a tissue microarray (TMA) from different phases of HNSCC development demonstrated increased expression of HOXD10 in primary tumours and loss of expression in metastases, similar to expression changes observed *in vitro* (Figure 1B and C). The OPL tissues (with a range of grades of dysplasia) demonstrate an intermediate pattern of HOXD10 expression, which is variable. Further analysis in TMA constructed from a cohort of 27 matched HNSCC primary tumours and metastases confirmed the pattern with

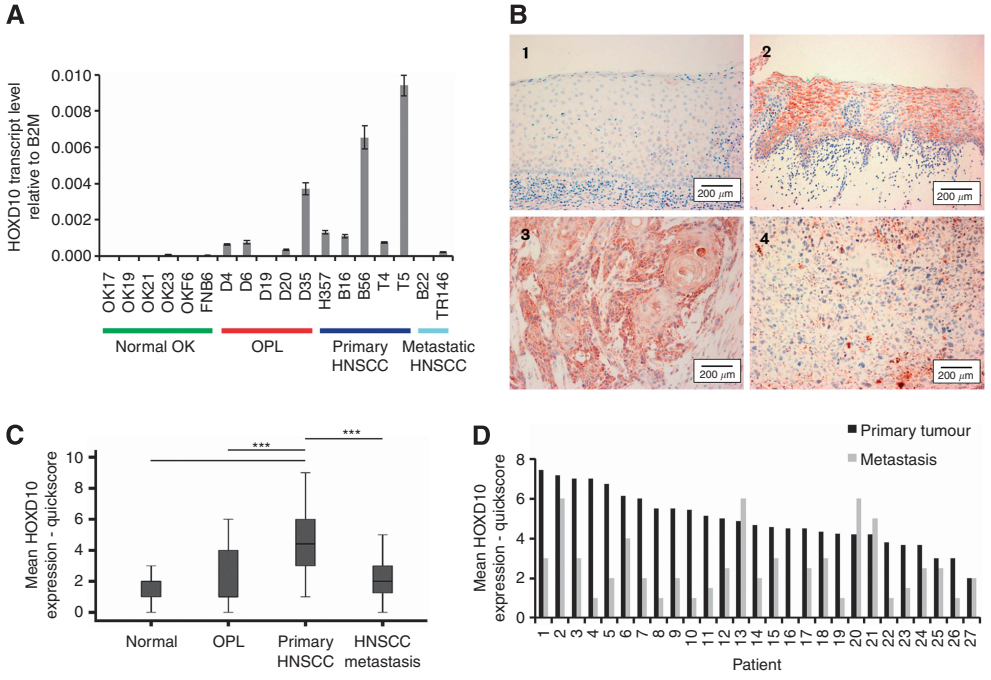

Figure 1. HOXD10 expression in a panel of normal, OPL and HNSCC cells and in HNSCC tissues. (**A**) HOXD10 expression in a panel of normal oral keratinocytes, oral premalignant lesion and HNSCC cell lines, assessed using qPCR. HOXD10 expression is high in primary HNSCC, low in HNSCC metastases and variable in OPLs. Each assay was conducted in triplicate and repeated three times. The data show the mean of triplicate repeats ± s.e.m. (**B**) Examples of expression of HOXD10 as assessed using IHC in normal, OPL and HNSCC tissues (from the cohort in **C**), demonstrating high expression in primary HNSCC. 1 is normal oral mucosa; 2 is OPL; 3 is primary HNSCC; and 4 is metastatic HNSCC. Photomicrograph overall magnification ×200, scale bar = 200 μm. (**C**) Overall IHC Quickscore of HOXD10 expression in the full cohort of tissues from normal mucosa ($n = 30$), OPL ($n = 18$), primary HNSCC ($n = 82$) and HNSCC metastases ($n = 27$). ***$P < 0.001$. (**D**) Mean Quickscore of HOXD10 expression assessed by IHC in a panel of 27 matched primary HNSCC with matched metastases. Expression of HOXD10 is lower in the metastasis in 23 out of 27 (85%) cases ($P < 0.05$).

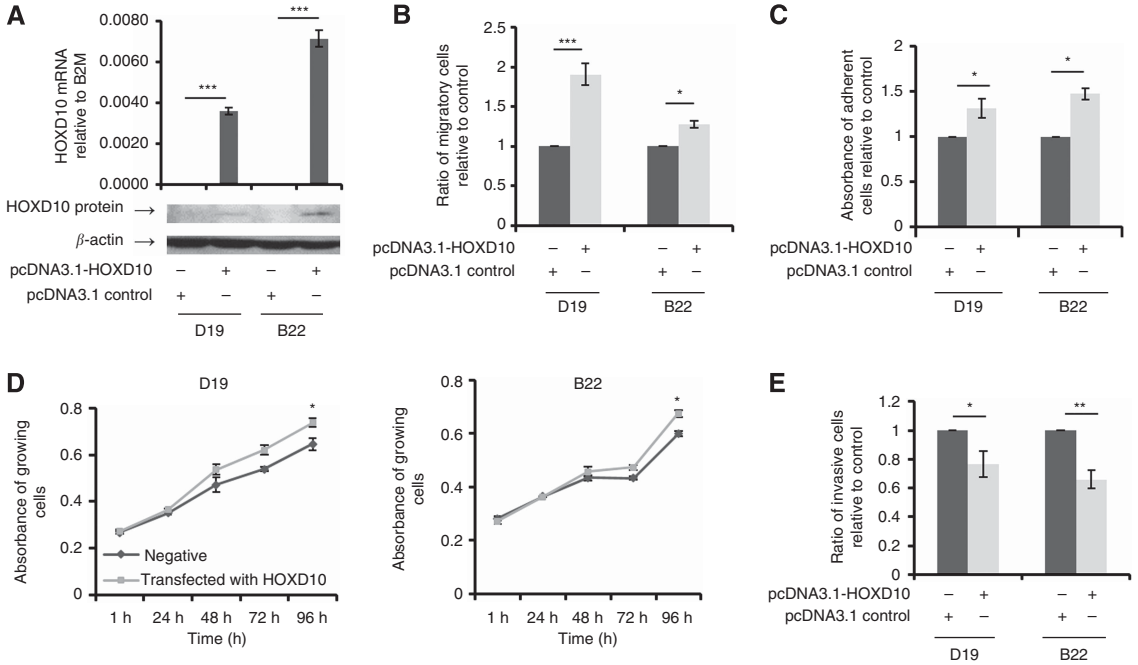

Figure 2. The effects of overexpression of HOXD10 in low-HOXD10-expressing OPL and HNSCC cells. (**A**). Expression of HOXD10 assessed using qPCR and WB, confirming raised expression in the transfected cells, compared with empty vector-transfected controls. β-actin is used as a loading control in WB. (**B–D**). Increasing HOXD10 expression in D19 and B22 increases migration in the Transwell assay (**B**), increases adhesion to fibronectin (**C**) and increases proliferation as assessed by MTS assay over 96 h (**D**). (**E**) Increasing HOXD10 expression in D19 and B22 reduces invasion into matrigel. *$P < 0.05$, ***$P < 0.001$. Each assay was conducted in triplicate and repeated three times. The data show the mean of triplicate repeats ± s.e.m.

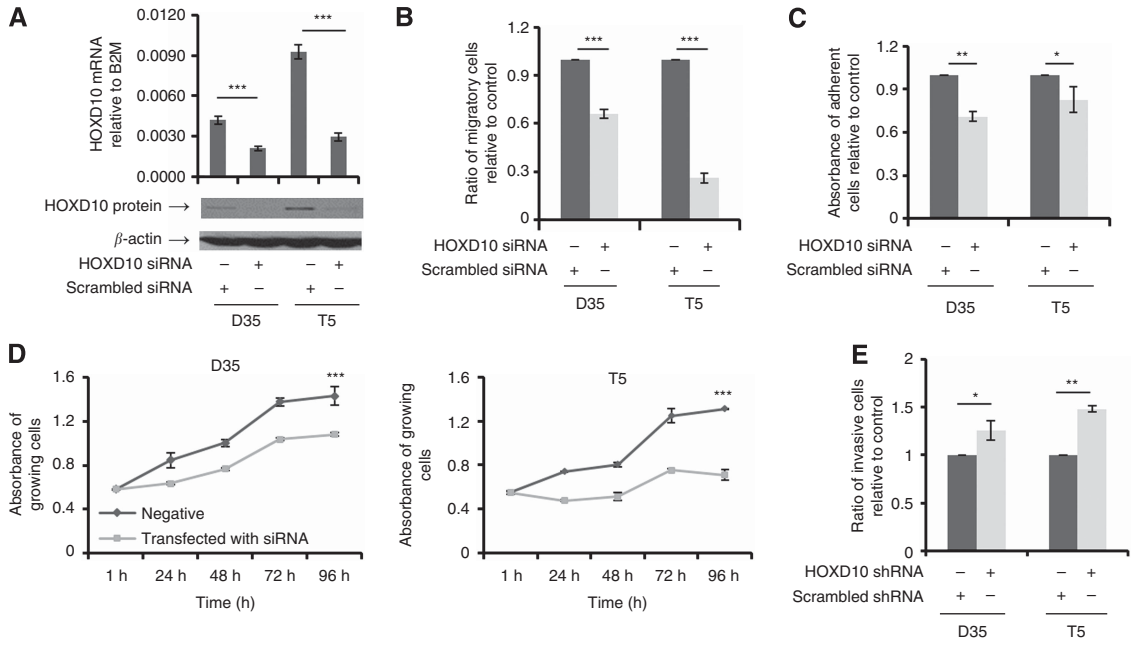

Figure 3. The effects of reduced expression of HOXD10 in high-HOXD10-expressing OPL and HNSCC cells. (**A**). Expression of HOXD10 assessed using qPCR and WB, confirming reduction in expression of HOXD10 in the transfected cells, compared with scrambled siRNA-transfected controls. β-actin is used as a loading control in WB. (**B–D**) Reducing HOXD10 expression in D35 and T5 cells reduces migration in the Transwell assay (**B**), reduces adhesion to fibronectin (**C**) and reduces proliferation as assessed by the MTS assay over 96 h (**D**). (**E**) Reducing HOXD10 expression in D35 and T5 increases invasion into matrigel. $*P<0.05$, $**P<0.01$, $***P<0.001$. Each assay was conducted in triplicate and repeated three times. The data show the mean of triplicate repeats ± s.e.m.

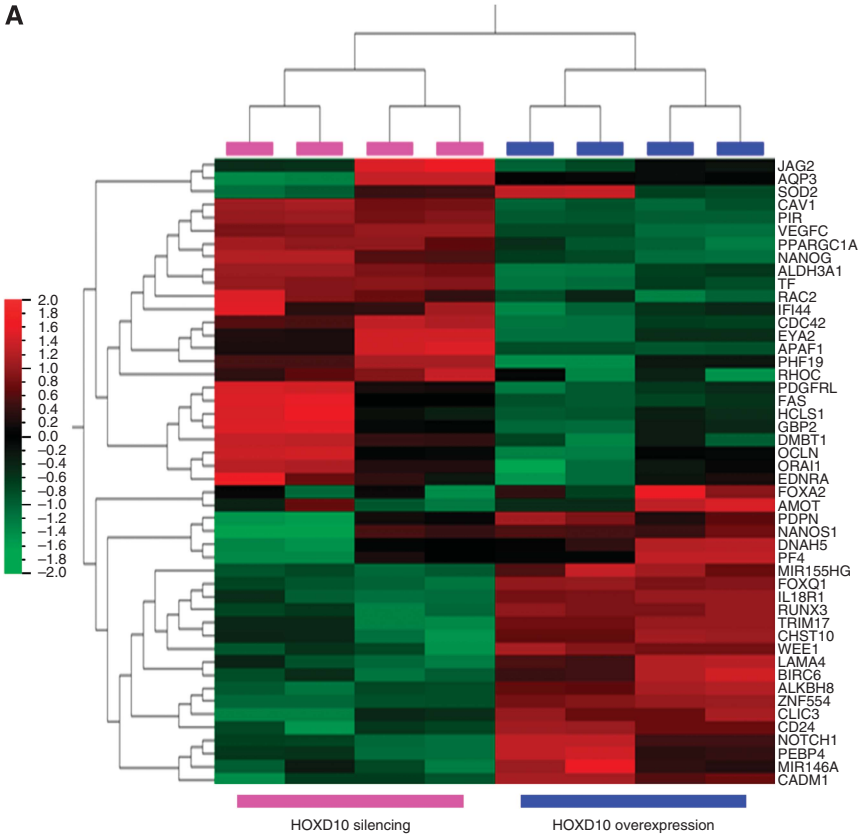

B

GENE	Correlation with HOXD10	Examples of reported roles/differential expression
AMOT	+	Promotes the proliferation of mammary epithelial cells (8) and regulates endothelial cell migration and linked to angiogenesis. (9)
CD24	+	Depletion of CD24 reduced cell proliferation, adhesion, and enhanced apoptosis (10) and contributes to tumour growth in urothelial carcinoma. (11)
CLIC3	+	Elevated in breast cancer in comparison with normal breast tissue and drive cancer progression. (12)
AQP3	+	Important for growth of oesophageal and oral squamous cell carcinoma. (13)
JAG2	+	Highly expressed in tongue carcinoma compared with normal tissues (14)
PDGFRL	−	Putative tumour suppressor in colorectal cancer cells. (15)
miR-155	−	Downregulated in gastric cancer cells and involved in metastasis. (16)
miR-146a	−	Inhibits cell growth, cell migration and induces apoptosis in non-small cell lung cancer cells. (17)

Figure 4. Expression microarray analysis identifies novel putative targets of HOXD10. (**A**) Heat map from the microarray data showing the top 48 differentially expressed genes on manipulation of HOXD10 expression (one-1way ANOVA, Benjamini–Hochberg corrected P-value <0.05, overall fold change >2). Red = high expression, green = low expression. The full list of these genes can be found in Supplementary Table S1. (**B**) Final list of putative HOXD10 targets, filtered by correlation (positive or negative) with HOXD10 expression.

expression lower in the metastases of 23 out of 27 patients (85%; Figure 1D).

Effects of manipulation of HOXD10 expression. First, we assessed the phenotypic consequences of transfecting HOXD10 into low-HOXD10-expressing OPL and metastatic HNSCC cells. Stable overexpression of HOXD10 was achieved in two cell lines, D19 (OPL) and B22 (metastasis), and confirmed using both qPCR and western blot analyses (Figure 2A). Increasing the expression of HOXD10 resulted in an increase in migration, adhesion to fibronectin and cell proliferation (Figure 2B–D) but a decrease in cell invasion (Figure 2E). The proportion of apoptotic cells in D19 was unchanged; however, a small increase was seen in B22 (Supplementary Figure S3A and B). Conversely, knockdown of HOXD10 was achieved using siRNA and confirmed using qPCR in high-HOXD10-expressing D35 (OPL) and T5 (HNSCC) cells (Figure 3A). This resulted in a decrease in migration, adhesion to fibronectin and proliferation, and an increase in invasion (Figure 3B–E), eliciting opposite effects to those seen on HOXD10 overexpression. There was no change in the proportion of apoptotic cells (Supplementary Figure S3C and D).

Microarray analysis of transfected cells. To identify the pathways and individual genes through which HOXD10 exerts these effects, we conducted expression microarray analysis of cells with stable HOXD10 overexpression (D19+ and B22+) or knockdown (D35− and T5−). After normalisation, data analysis yielded 9167 genes whose expression was significantly reciprocally altered in HOXD10-overexpressing and siRNA-transfected cells. The list was refined to 414 genes, using an overall fold change of >2. Gene ontology (GO) mapping of the differentially expressed genes identified a number of significantly enriched GO categories (Supplementary Table S1). These map to the effects seen in the cells on the manipulation of HOXD10.

Validation of putative HOXD10 target genes. After further filtering by *in silico* analysis, a final list of 48 differentially expressed genes were identified as putative targets of HOXD10 (Figure 4A; Supplementary Table S2). Using qPCR analysis, the expression level of the selected 48 HOXD10 putative targets were assessed in the manipulated cells and also in the whole panel of cell lines (data not shown). Thirty-nine of these genes showed a negative or positive correlation between their expression and

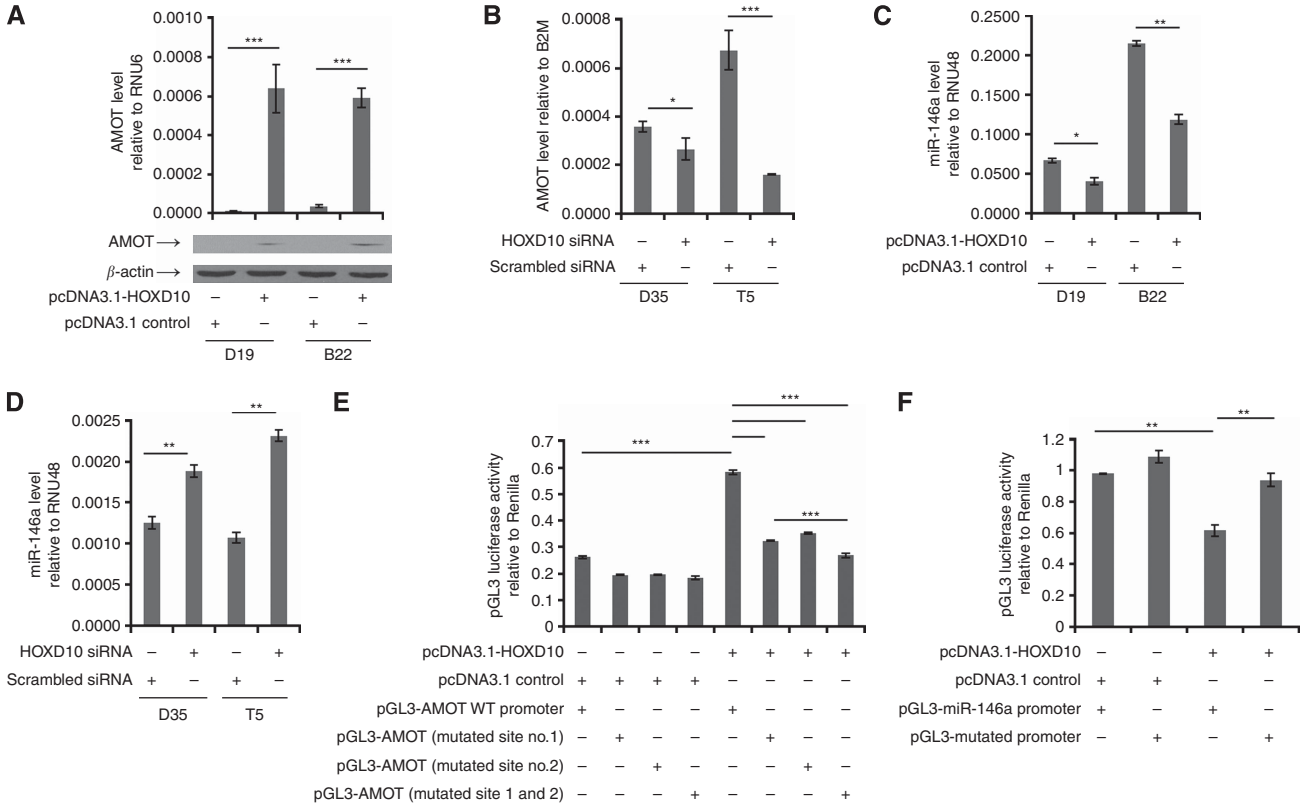

Figure 5. Validation of the microarray data for AMOT-p80 and miR-146a and confirmation of direct effect of HOXD10 on expression. (**A**) Expression of AMOT-p80 assessed by qPCR and WB, confirming raised expression in the HOXD10-transfected cells, compared with empty vector-transfected controls. β-actin is used as a loading control. (**B**) Expression of AMOT-p80 assessed using qPCR, confirming reduced expression in the HOXD10 siRNA-transfected cells, compared with scrambled siRNA controls. (**D**) Expression of miR-146a assessed using qPCR, confirming increased expression in the HOXD10 siRNA-transfected cells, compared with scrambled siRNA controls. (**E**) pGL3 luciferase reporter vectors containing either WT AMOT promoter, AMOT promoter with either mutated HOXD10 binding sites or AMOT promoter with both mutated binding sites were transfected into D19 cells stably transfected with either pcDNA3.1-HOXD10 or pcDNA3.1 control plasmids. DLR analysis shows that HOXD10 increases luciferase expression when pGL3 vector contains WT promoter. However, luciferase expression decreases when either of HOXD10-binding sites in AMOT promoter were mutated. No significant reduction in luciferase expression was detected when both mutated sites existed in the same pGL3 vector compared with pGL3 vector containing only one mutated binding site. $^{**}P<0.01$, each assay was conducted in triplicate and repeated three times. Data show the mean of triplicate repeats ± s.e.m. (**C**) Expression of miR-146a assessed using qPCR, confirming reduced expression in the HOXD10-transfected cells, compared with empty vector-transfected controls. (**F**) pGL3 luciferase reporter vectors containing either WT miR-146a promoter or miR-146a promoter with a mutated HOXD10-binding site were transfected into D19 cells stably transfected with either pcDNA3.1-HOXD10 or pcDNA3.1 control plasmid. DLR analysis shows that HOXD10 increases luciferase expression when pGL3 vector contains WT promoter. However, luciferase expression decreases when either of HOXD10-binding sites in miR-146a promoter was mutated. $^{**}P<0.01$, each assay was conducted in triplicate and repeated three times. Data show the mean of triplicate repeats ± s.e.m.

HOXD10 expression in both HOXD10-manipulated cells and a panel of cell lines. The top eight differentially expressed genes are shown in Figure 4B, selected on the basis of close relation to HOXD10 expression and *in silico* analysis for putative HOXD10-binding sites in the promoter; the two candidates that most closely matched HOXD10 expression were angiomotin (transcript variant 2, AMOT-p80) and miR-146a.

Immunoblotting showed that AMOT-p80 protein expression increased after HOXD10 transfection in low expressing OPM and HNSCC cells (Figure 5A) but was reduced in high-expressing (D35 and T5) cells transfected with HOXD10 siRNA (Figure 5B), in keeping with the microRNA data. AMOT-p80 expression was also assessed in a wider panel of NOKs, OPL and HNSCC cells, showing a pattern of expression that is similar to that of HOXD10 (Supplementary Figure S5C and D). miR-146a expression decreased after HOXD10 transfection in low expressing OPL and HNSCC cells (Figure 5C) and was induced after HOXD10 siRNA transfection into high-expressing cells (Figure 5D). miR-146a expression was also assessed in the same panel of NOKs, OPL and HNSCC cells, showing high expression in normal cells, and low expression in HNSCC cells, which suggests a negative correlation with HOXD10 expression level (Supplementary Figure S5A and B).

Investigation of AMOT-p80 and miR-146a promoters as direct targets of HOXD10. HOXD10 overexpression increased luciferase activity from a wild-type AMOT-p80 promoter reporter construct (Figure 5E). This was not observed after mutation of the putative HOXD10-binding sites in the promoter (Figure 5E), indicating a direct effect of HOXD10 on AMOT-p80 expression at a transcriptional level. The effect was further increased by mutating more than one HOXD10-binding site. HOXD10 overexpression suppressed luciferase activity from a wild-type miR-146 promoter reporter construct (Figure 5F). This was not observed after mutation of the putative HOXD10-binding site (Figure 5F), indicating that HOXD10 directly suppresses miR-146a expression by interacting with its promoter.

The function of AMOT-p80 in HNSCC cells. Transient transfection of AMOT-p80 into HNSCC cells that express low levels of HOXD10 and AMOT (B22 and D19, expression confirmed using qPCR and WB in Figure 6A) resulted in similar phenotypic changes to transfection with HOXD10; there was an increase in proliferation and migration of cells (Figure 6B and C). There was no effect on adhesion to fibronectin (Figure 6D).

Transfection of AMOT-p80 into cells stably depleted of HOXD10 (Figure 7A) rescued the phenotype, with partial reversal of the reduction in proliferation (Figure 7B) and reversion of migration to a level higher than original control levels (Figure 7C). Assessment of expression of AMOT-p80 in a panel of normal oral mucosa and HNSCC tissues showed that the expression of AMOT-p80 was much higher in the HNSCC samples, where there was both cytoplasmic and nuclear expression of AMOT-p80 (in keeping with a recent report in hepatocellular tumorigenesis (Yi *et al*, 2013)) with focal light cytoplasmic expression in normal oral mucosa (Figure 7D).

DISCUSSION

Various HOX genes have been described to have a role in the development of a wide range of cancers. The role of HOXA cluster genes in haematolymphoid cancers has been extensively investigated, resulting in the identification of a number of fusion proteins (for example, NUP98 : HOXC11) that results in aberrant HOX *trans*-regulatory activity. In primary breast cancers, HOXA5, HOXA9 and HOXB13 are downregulated, whereas HOXB9 and HOXD10 are upregulated (Chen *et al*, 2004; Ma *et al*, 2007; Gilbert *et al*, 2010). Changes in the expression of other HOX genes have been reported in lung and gastric cancers (Abe *et al*, 2006). In HNSCC, several HOX genes, including HOXA5, HOXD10 and HOXD11, show higher levels of expression in oral cancer tissues compared with normal tissues (Rodini *et al*, 2012). Although high expression levels of HOXD10 have previously been observed in

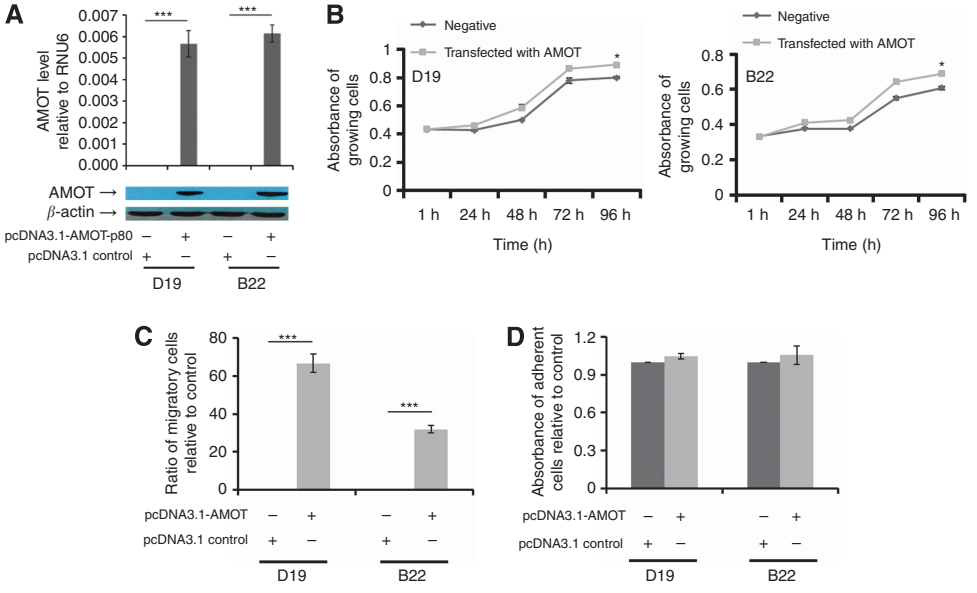

Figure 6. AMOT-p80 exerts similar phenotypic effects to that seen on manipulation of HOXD10. (**A**) Expression of AMOT-p80 assessed using qPCR and WB, confirming raised expression of AMOT-p80 in transfected cells, compared with empty vector-transfected controls. β-actin is used as a loading control. (**B**) Cell growth was assessed using the MTS assay over 96 h. Introducing AMOT into low-AMOT cells (D19, B22) has resulted in an increase in their proliferation. (**C**) D19 and B22 cells transfected with AMOT show an increase in migration in the Transwell assay compared with cells transfected with a control plasmid. (**D**) Assessing cell adhesion to a fibronectin-coated surface shows that introducing high levels of AMOT by transfection had no significant effect. *$P<0.05$, ***$P<0.001$, each assay was conducted in triplicate and repeated three times. Data show the mean of triplicate repeats ± s.e.m.

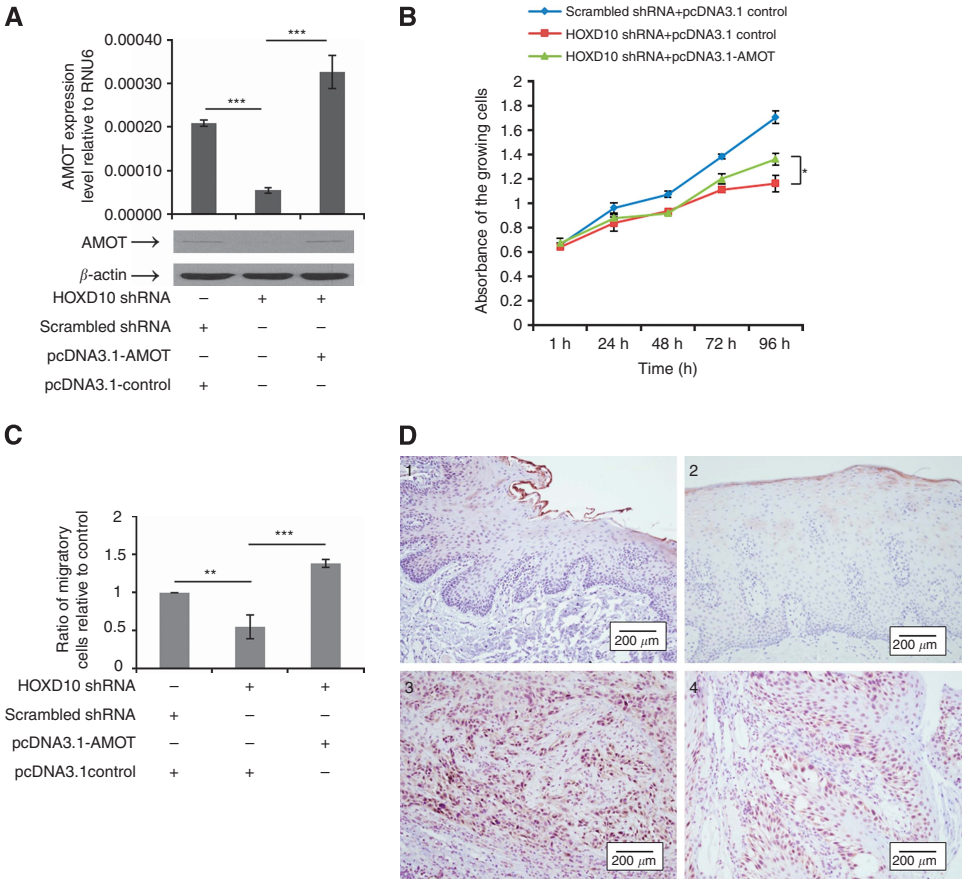

Figure 7. AMOT-p80 rescues the phenotype seen on knockdown of HOXD10 and is highly expressed in primary HNSCC. (**A**) Expression of AMOT assessed using qPCR and WB, confirming reduced expression in the HOXD10 shRNA stably transfected cells, and increased expression in AMOT-p80-transfected cells, compared with empty vector-transfected controls. β-actin is used as a loading control. (**B**) Knockdown of HOXD10 expression by siRNA in D19 and B22 increases proliferation as assessed using MTS assay over 96 h. This is partially rescued by the expression of AMOT in these cells. (**C**) Knockdown of HOXD10 expression in D19 and B22 reduces migration in the Transwell assay, and this is fully rescued by the overexpression of AMOT, to levels higher than controls. (**D**) Expression of AMOT as assessed using IHC in normal (1 and 2) and HNSCC tissues (3 and 4), demonstrating high expression in primary HNSCC. Photomicrograph overall magnification ×200. *$P<0.05$, **$P<0.01$, ***$P<0.001$, each assay was conducted in triplicate and repeated three times. Data show the mean of triplicate repeats ± s.e.m.

invasive oral cancers, this is the first study to explore the functional roles of HOXD10 in HNSCC development. We also demonstrate that HOXD10 expression is reduced in HNSCC metastases relative to their paired primary tumours.

We show that HOXD10 promotes the proliferation, migration and adhesion to fibronectin of primary HNSCC cells, with no consistent effect on apoptosis, by demonstrating reciprocal phenotypic changes on overexpression of knockdown of HOXD10. These effects may promote the development of the primary tumour as it becomes established at the primary site. This is supported by the observation that some OPL cells also express high levels of HOXD10. Thus, it is likely that increasing HOXD10 expression during HNSCC development supports the emergence of cells that populate the primary tumour. Interestingly, the observations that HOXD10 suppresses invasion into matrigel, that expression of HOXD10 is low in cells derived from metastases and that the tumour loses expression of HOXD10 in its metastases suggest a change in the role HOXD10 is having as cancer develops and spreads to sites distant to the primary tumour. Inhibition of invasion by HOXD10 would indicate antimetastatic properties, which have been demonstrated in other cancer types (Ma *et al*, 2010). The overall pattern of high primary tumour HOXD10 expression, with the loss of expression in metastases that we have observed, has been reported in other cancer types, such as bladder cancer (Baffa *et al*, 2009). Furthermore, in breast cancer, tumorigenic but nonmetastatic breast cancer cell lines express little or no miR-10b, which downregulates HOXD10 expression, in keeping with high HOXD10 expression (Ma *et al*, 2007). However, this does not seem to be a consistent pattern across all cancer types, as in primary gastric cancer types HOXD10 is downregulated by promoter methylation, which profoundly inhibits proliferation and migration (Wang *et al*, 2012). This highlights the context and cell-specific roles of these transcription factors, particularly as their expression may be regulated by a number of different mechanisms.

In breast and gastric cancer cells, high expression of miR-10b activates signalling via the RhoC-AKT signalling pathway that promotes migration and invasion (Ma *et al*, 2007; Liu *et al*, 2012). Our phenotypic assessment of the effects of HOXD10 in HNSCC cells indicates that low expression of HOXD10 is associated with increased invasive potential and the expression microarray analysis of these cells indicates that low HOXD10 expression increases the expression of a number of known modulators of epithelial–mesenchymal transition (EMT; Supplementary Figure S4 and Supplementary Table S2). Indeed, recent investigations in stem cell programming and cancer have demonstrated that miR-10b (and other microRNAs) modulates EMT (Han *et al*, 2014), which is also known to be an important part of the pro-metastatic phenotype cancer cells derive as they develop. The direct link to HOXD10, however, has not been made in this context.

The mechanism of downregulation of HOXD10 in HNSCC as it metastasises is not clear. In contrast to that seen in breast and ovarian cancer, there is no direct relationship between the expression of HOXD10 and miR-10b in HNSCC, (Supplementary Figure S2), in keeping with other work in the field (Severino *et al*, 2013). Our unpublished observations also suggest that downregulation is not due to promoter methylation in these HNSCC cells (data not shown). Thus, there is scope for further investigation of other potential mechanisms of modulation of HOXD10 in keratinocytes, both in terms of the initiating promotion of expression and its subsequent loss in lymph node metastases. Other suggestions include the possible role of long non-coding RNAs such as HOTAIR; however, these effects also appear to be tumour-specific (Nakayama *et al*, 2013).

The differential pattern of expression observed here poses interesting questions regarding the possible uses of HOXD10 both as a biomarker and as a potential therapeutic target. Of the tumours that metastasised, all demonstrated the pattern of high expression in the primary tumour and low expression in metastases. No significant association of the loss of HOXD10 expression in the primary tumour with the presence of metastasis was identified; thus, it is unlikely to be useful as a prognostic biomarker. Similarly, it is not likely to be a potential therapeutic target in itself, as both high and low expression, in the correct context, can support development and progression of the tumour. Nevertheless, its possible utility as a marker of progression of OPLs to HNSCC warrants further investigation, given the high expression in some OPL cells and tissues that may be related to the risk of progression to invasive disease. In addition, as HOXD10 is acting as a transcription factor, identification of the targets of HOXD10 at the particular stage of disease development indicated may identify useful biomarkers or novel therapeutic targets.

We used expression microarray analysis to identify possible targets of HOXD10. Although this approach has acknowledged limitations, our algorithm for target identification was successful in the identification of a number of novel direct HOXD10 targets, including angiomotin (AMOT-p80) and miR-146a.

miR-146a is well established as an inhibitor of cell proliferation and as a suppressor of metastasis (Hurst *et al*, 2009; Chen *et al*, 2013; Yao *et al*, 2013), and thus the finding that HOXD10 decreases miR-146a expression is in keeping with the observed phenotype. We therefore conducted detailed investigation on the role of the novel identified target, AMOT-p80, understanding of which in the context of cancer biology is limited.

The angiomotin family of proteins, in which there are three members (AMOT, AMOTL1 and AMOTL2), belongs to the motin family of angiostatin-binding proteins and is involved in the regulation of cell growth and motility. They have been localised in close association with tight junctions, whose enhanced turnover has been associated with promotion of tumour development in HNSCC (Vilen *et al*, 2012). Two isoforms of AMOT have been identified (p80 and p130), with the increased expression of AMOT-p80 associated with increased migration of endothelial cells (Ernkvist *et al*, 2008). The activity of AMOT-p80 is inhibited by the 4.1 protein superfamily member, Merlin, in a complex at tight junctions which includes YAP, LATS and other AMOT family members (Paramasivam *et al*, 2011). Recent investigations have demonstrated that AMOT-p80 opposes the activation of signalling pathways by other AMOT family members, including activation of tumour suppressors YAP and LATS2 (Zhao *et al*, 2011). Others have shown that AMOT-p80 promotes tumour growth in a number of different contexts: signalling via RAS-MAPK to promote both proliferation of embryonal kidney cell lines and enhanced development of xenograft tumours in mice using NF2 null Schwann cells (Yi *et al*, 2011); signalling via ERK1/2 in breast cancer cells, resulting in increased proliferation and dysregulated cell polarity that resulted in a more neoplastic growth pattern (Ranahan *et al*, 2011). Our data in HNSCC support the role of AMOT-p80 in the promotion of tumour growth, although it is not clear whether HOXD10 has a role in control of AMOT-p80 expression in these other tumour types. Nevertheless, AMOT-p80 is a potential target for novel therapeutics that may be useful in a number of cancer types. Both AMOT-p80 and miR-146a, identified here as novel HOXD10 targets, may represent therapeutic targets at particular tumour-promoting stages.

ACKNOWLEDGEMENTS

We would like to thank Dr Adam Jones and Mrs Ibtisam Zargoun for the TMAs in this project and Dr Helen Colley for her assistance with the apoptosis assays. FH is supported by the Government of the Kingdom of Saudi Arabia.

CONFLICT OF INTEREST

The authors declare no conflict of interest.

REFERENCES

Abe M, Hamada J, Takahashi O, Takahashi Y, Tada M, Miyamoto M, Morikawa T, Kondo S, Moriuchi T (2006) Disordered expression of HOX genes in human non-small cell lung cancer. *Oncol Rep* **15**(4): 797–802.

Agrawal N, Frederick MJ, Pickering CR, Bettegowda C, Chang K, Li RJ, Fakhry C, Xie TX, Zhang J, Wang J, Zhang N, El-Naggar AK, Jasser SA, Weinstein JN, Trevino L, Drummond JA, Muzny DM, Wu Y, Wood LD, Hruban RH, Westra WH, Koch WM, Califano JA, Gibbs RA, Sidransky D, Vogelstein B, Velculescu VE, Papadopoulos N, Wheeler DA, Kinzler KW, Myers JN (2011) Exome sequencing of head and neck squamous cell carcinoma reveals inactivating mutations in NOTCH1. *Science* **333**(6046): 1154–1157.

Baffa R, Fassan M, Volinia S, O'Hara B, Liu CG, Palazzo JP, Gardiman M, Rugge M, Gomella LG, Croce CM, Rosenberg A (2009) MicroRNA expression profiling of human metastatic cancers identifies cancer gene targets. *J Pathol* **219**(2): 214–221.

Cartharius K, Frech K, Grote K, Klocke B, Haltmeier M, Klingenhoff A, Frisch M, Bayerlein M, Werner T (2005) MatInspector and beyond: promoter analysis based on transcription factor binding sites. *Bioinformatics* **21**(13): 2933–2942.

Chen G, Umelo IA, Lv S, Teugels E, Fostier K, Kronenberger P, Dewaele A, Sadones J, Geers C, De Greve J (2013) miR-146a inhibits cell growth, cell migration and induces apoptosis in non-small cell lung cancer cells. *PLoS One* **8**(3): e60317.

Chen H, Chung S, Sukumar S (2004) HOXA5-induced apoptosis in breast cancer cells is mediated by caspases 2 and 8. *Mol Cell Biol* **24**(2): 924–935.

Detre S, Saclani Jotti G, Dowsett M (1995) A "quickscore" method for immunohistochemical semiquantitation: validation for oestrogen receptor in breast carcinomas. *J Clin Pathol* **48**(9): 876–878.

Eklund EA (2007) The role of HOX genes in malignant myeloid disease. *Curr Opin Hematol* **14**(2): 85–89.

Ernkvist M, Birot O, Sinha I, Veitonmaki N, Nystrom S, Aase K, Holmgren L (2008) Differential roles of p80- and p130-angiomotin in the switch between migration and stabilization of endothelial cells. *Biochim Biophys Acta* **1783**(3): 429–437.

Gilbert PM, Mouw JK, Unger MA, Lakins JN, Gbegnon MK, Clemmer VB, Benezra M, Licht JD, Boudreau NJ, Tsai KK, Welm AL, Feldman MD, Weber BL, Weaver VM (2010) HOXA9 regulates BRCA1 expression to modulate human breast tumor phenotype. *J Clin Invest* **120**(5): 1535–1550.

Halees AS, Leyfer D, Weng Z (2003) PromoSer: A large-scale mammalian promoter and transcription start site identification service. *Nucleic Acids Res* **31**(13): 3554–3559.

Han X, Yan S, Weijie Z, Feng W, Liuxing W, Mengquan L, Qingxia F (2014) Critical role of miR-10b in transforming growth factor-beta1-induced epithelial-mesenchymal transition in breast cancer. *Cancer Gene Ther* **21**(2): 60–67.

Hearnden V, Lomas H, Macneil S, Thornhill M, Murdoch C, Lewis A, Madsen J, Blanazs A, Armes S, Battaglia G (2009) Diffusion studies of nanometer polymersomes across tissue engineered human oral mucosa. *Pharm Res* **26**(7): 1718–1728.

Hunter KD, Thurlow JK, Fleming J, Drake PJ, Vass JK, Kalna G, Higham DJ, Herzyk P, Macdonald DG, Parkinson EK, Harrison PR (2006) Divergent routes to oral cancer. *Cancer Res* **66**(15): 7405–7413.

Hurst DR, Edmonds MD, Scott GK, Benz CC, Vaidya KS, Welch DR (2009) Breast cancer metastasis suppressor 1 up-regulates miR-146, which suppresses breast cancer metastasis. *Cancer Res* **69**(4): 1279–1283.

Leemans CR, Braakhuis BJ, Brakenhoff RH (2011) The molecular biology of head and neck cancer. *Nat Rev Cancer* **11**(1): 9–22.

Liu Z, Zhu J, Cao H, Ren H, Fang X (2012) miR-10b promotes cell invasion through RhoC-AKT signaling pathway by targeting HOXD10 in gastric cancer. *Int J Oncol* **40**(5): 1553–1560.

Ma L, Reinhardt F, Pan E, Soutschek J, Bhat B, Marcusson EG, Teruya-Feldstein J, Bell GW, Weinberg RA (2010) Therapeutic silencing of miR-10b inhibits metastasis in a mouse mammary tumor model. *Nat Biotechnol* **28**(4): 341–347.

Ma L, Teruya-Feldstein J, Weinberg R (2007) Tumour invasion and metastasis initiated by microRNA-10b in breast cancer. *Nature* **449**(7163): 682–688.

Messeguer X, Escudero R, Farre D, Nunez O, Martinez J, Alba MM (2002) PROMO: detection of known transcription regulatory elements using species-tailored searches. *Bioinformatics* **18**(2): 333–334.

Morgan R, Boxall A, Harrington KJ, Simpson GR, Gillett C, Michael A, Pandha HS (2012) Targeting the HOX/PBX dimer in breast cancer. *Breast Cancer Res Treat* **136**(2): 389–398.

Nakayama I, Shibazaki M, Yashima-Abo A, Miura F, Sugiyama T, Masuda T, Maesawa C (2013) Loss of HOXD10 expression induced by upregulation of miR-10b accelerates the migration and invasion activities of ovarian cancer cells. *Int J Oncol* **43**(1): 63–71.

Paramasivam M, Sarkeshik A, Yates JR, Fernandes MJG, McCollum D (2011) Angiomotin family proteins are novel activators of the LATS2 kinase tumor suppressor. *Mol Biol Cell* **22**(19): 3725–3733.

Picchi J, Trombi L, Spugnesi L, Barachini S, Maroni G, Brodano GB, Boriani S, Valtieri M, Petrini M, Magli MC (2013) HOX and TALE signatures specify human stromal stem cell populations from different sources. *J Cell Physiol* **228**(4): 879–889.

Pickering CR, Zhang J, Yoo SY, Bengtsson L, Moorthy S, Neskey DM, Zhao M, Ortega Alves MV, Chang K, Drummond J, Cortez E, Xie TX, Zhang D, Chung W, Issa JP, Zweidler-McKay PA, Wu X, El-Naggar AK, Weinstein JN, Wang J, Muzny DM, Gibbs RA, Wheeler DA, Myers JN, Frederick MJ (2013) Integrative genomic characterization of oral squamous cell carcinoma identifies frequent somatic drivers. *Cancer Discov* **3**(7): 770–781.

Ranahan WP, Han Z, Smith-Kinnaman W, Nabinger SC, Heller B, Herbert BS, Chan R, Wells CD (2011) The adaptor protein AMOT promotes the proliferation of mammary epithelial cells via the prolonged activation of the extracellular signal-regulated kinases. *Cancer Res* **71**(6): 2203–2211.

Rice KL, Licht JD (2007) HOX deregulation in acute myeloid leukemia. *J Clin Invest* **117**(4): 865–868.

Rinn JL, Kertesz M, Wang JK, Squazzo SL, Xu X, Brugmann SA, Goodnough LH, Helms JA, Farnham PJ, Segal E, Chang HY (2007) Functional demarcation of active and silent chromatin domains in human HOX loci by Noncoding RNAs. *Cell* **129**(7): 1311–1323.

Rodini CO, Xavier FC, Paiva KB, De Souza Setubal Destro MF, Moyses RA, Michaluarte P, Carvalho MB, Fukuyama EE, Head Neck, Genome Project G, Tajara EH, Okamoto OK, Nunes FD (2012) Homeobox gene expression profile indicates HOXA5 as a candidate prognostic marker in oral squamous cell carcinoma. *Int J Oncol* **40**(4): 1180–1188.

Severino P, Bruggemann H, Andreghetto FM, Camps C, Klingbeil Mde F, de Pereira WO, Soares RM, Moyses R, Wunsch-Filho V, Mathor MB, Nunes FD, Ragoussis J, Tajara EH (2013) MicroRNA expression profile in head and neck cancer: HOX-cluster embedded microRNA-196a and microRNA-10b dysregulation implicated in cell proliferation. *BMC Cancer* **13**: 533.

Smith PK, Krohn RI, Hermanson GT, Mallia AK, Gartner FH, Provenzano MD, Fujimoto EK, Goeke NM, Olson BJ, Klenk DC (1985) Measurement of protein using bicinchoninic acid. *Anal Biochem* **150**(1): 76–85.

Vilen ST, Suojanen J, Salas F, Risteli J, Ylipalosaari M, Itkonen O, Koistinen H, Baumann M, Stenman UH, Sorsa T, Salo T, Nyberg P (2012) Trypsin-2 enhances carcinoma invasion by processing tight junctions and activating ProMT1-MMP. *Cancer Invest* **30**(8): 583–592.

Wang LJ, Chen SJ, Xue M, Zhong J, Wang X, Gan LH, Lam EKY, Liu X, Zhang JB, Zhou TH, Yu J, Jin HC, Si JM (2012) Homeobox D10 gene, a candidate tumor suppressor, is downregulated through promoter hypermethylation and associated with gastric carcinogenesis. *Mol Med* **18**(3): 389–400.

Wardwell-Ozgo J, Dogruluk T, Gifford A, Zhang Y, Heffernan TP, van Doorn R, Creighton CJ, Chin L, Scott KL (2014) HOXA1 drives melanoma tumor growth and metastasis and elicits an invasion gene expression signature that prognosticates clinical outcome. *Oncogene* **33**(8): 1017–1026.

Wu X, Chen H, Parker B, Rubin E, Zhu T, Lee JS, Argani P, Sukumar S (2006) HOXB7, a homeodomain protein, is overexpressed in breast cancer and confers epithelial-mesenchymal transition. *Cancer Res* **66**(19): 9527–9534.

Yao Q, Cao Z, Tu C, Zhao Y, Liu H, Zhang S (2013) MicroRNA-146a acts as a metastasis suppressor in gastric cancer by targeting WASF2. *Cancer Lett* **335**(1): 219–224.

Yi CL, Shen ZW, Stemmer-Rachamimov A, Dawany N, Troutman S, Showe LC, Liu Q, Shimono A, Sudol M, Holmgren L, Stanger BZ, Kissil JL (2013) The p130 isoform of angiomotin is required for Yap-mediated hepatic epithelial cell proliferation and tumorigenesis. *Science Signaling* **6**(291): ra77.

Yi CL, Troutman S, Fera D, Stemmer-Rachamimov A, Avila JL, Christian N, Persson NL, Shimono A, Speicher DW, Marmorstein R, Holmgren L, Kissil JL (2011) A tight junction-associated merlin-angiomotin complex mediates merlin's regulation of mitogenic signaling and tumor suppressive functions. *Cancer Cell* **19**(4): 527–540.

Zhang MQ (2003) Prediction, annotation, and analysis of human promoters. *Cold Spring Harbor Symp Quant Biol* **68**: 217–225.

Zhao B, Li L, Lu Q, Wang LH, Liu CY, Lei QY, Guan KL (2011) Angiomotin is a novel Hippo pathway component that inhibits YAP oncoprotein. *Gene Dev* **25**(1): 51–63.

Ziegler EC, Ghosh S (2005) Regulating inducible transcription through controlled localization. *Sci STKE* **2005**(284): re6.

Supplementary Information accompanies this paper on British Journal of Cancer website (http://www.nature.com/bjc)